Spatial insights of lung pathology in COVID-19 autopsies

Domenic Abbondanza, Asa Segerstolpe, Yiming Yang, Malika Sud, Jonathan Chen, Robin Fropf, Marty Ross,

Sarah Warren, Prajan Divakar, Joseph Beechem, Samouil L Farhi, Isaac Solomon, Bo Li, Orit Rozenblatt-Rosen, Aviv Regev

Abstract

COVID-19, the disease caused by the novel severe acute respiratory syndrome coronavirus 2 (SARS-CoV-2), is a global health threat due to its rapid spread, morbidity, and mortality. A primary cause of death from SARS-CoV-2 infection is respiratory failure. Therefore, there is an urgent and critical need to identify the drivers of lung pathology in patients with severe SARS-CoV-2 lung infection. We surveyed lung tissues from 9 COVID-19 rapid autopsy donors and 3 uninfected control lungs with the NanoString GeoMx® Digital Spatial Profiling (DSP) platform. We first screened our tissues using RNAscope probe targeting the SARS-CoV-2 genome and showed strong inter- and intra-individual differences in viral load. Guided by the observed level of viral signal, we performed comprehensive spatial profiling of pathological lung regions with the GeoMx Cancer Transcriptome Atlas (CTA, 1,822-plex) and Whole Transcriptome Atlas (WTA, 18,154-plex) RNA assays with next generation sequencing (NGS) readout, as well as the GeoMx protein assay (83-plex) with nCounter readout. We sampled 198 regions across all samples, 133 of which were further segmented with the epithelial morphology marker pan cytokeratin (PanCK). We detected enriched viral transcripts, inflammatory chemokines and cytokines, and interferon induced genes within PanCK$^+$ areas of high viral load. Moreover, we transcriptionally profiled single-cells and single-nuclei from 4 COVID-19 autopsy lungs from the same cohort, and 13 from other COVID-19 autopsy cohorts, and used this data to deconvolve and increase the resolution of our spatial profiling. With this rich dataset, we were able to characterize the intra-pulmonary heterogeneity and molecular changes caused by the infection, and point to putative molecular pathways involved in COVID-19 disease pathogenesis.

Nanostring DSP workflow

Process: Tissue is prepared via conventional ISH protocol and incubated with RNA detection probes, labeled by fluorescently-conjugated antibodies and a nucleic acid stain for visualization.

View: Areas of interest (AOIs) are identified with fluorescence imaging.

Profile: Selected AOIs are chosen for high-resolution multiplex profiling, and oligos from the selected region are released upon exposure to UV light.

Collection: Photocleaved oligos are then collected via a microcapillary tube and stored in a microplate well

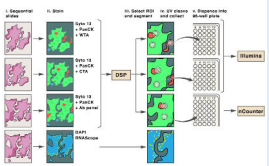

Digital counting: Photocleaved oligos from the spatially-resolved ROIs in the microplate are hybridized to 4-color, 6-spot optical barcodes, enabling up to ~1 million digital counts of the targets (distributed across all targets) in a single AOI using standard NanoString nCounter® instruments or Illumina sequencing platforms.

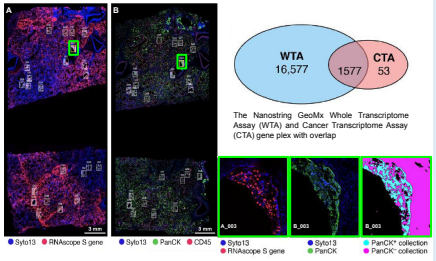

The GeoMx instrument's capability of high resolution whole slide scanning allows for accurate, reproducible placement of AOIs between serial tissue sections

The Nanostring GeoMx Whole Transcriptome Assay (WTA) and Cancer Transcriptome Assay (CTA) gene plex with overlap

A single AOI, segmented based on RNAscope S gene probe (left) and PanCK (middle, right)

COVID-19 autopsy cohort

	No	Broad ID	Race	Ethnicity	Sex	Age	CTA	WTA	Protein	Processed for sn/scRNA-Seq	Organ failure	S/s to death (days)
COVID-19 negative	D20	04-P716490	White	Not Hispanic/ Latino	M	50-55	Parenchyma	Parenchyma	Parenchyma	No	Multi-organ	9
	D20	04-P809371	Black/ AA	Not Hispanic/ Latino	F	70-80	Parenchyma	Parenchyma	Parenchyma	No	Heart	8
	D24	04-P979210	White	Not Hispanic/ Latino	M	50-55	Parenchyma	Parenchyma	Parenchyma	No	Multi-organ	5
COVID-19 positive	D16	04-P910577	Black/ AA	–	F	65-70	Lung-LUL	Lung-LUL, -RUL	Lung-LUL	No	Lung	10
	D19	04-P439472	Other	Hispanic/ Latino	M	55-60	Lung-LUL	Lung-LUL, -LLL	Lung-LUL	No	Lung	6
	D23	04-P478538	White	–	F	65-70	Lung-LUL, trachea	Lung-LUL, heart-LV	Lung-LUL	No	Lung, heart	1
	D21	04-P541935	–	Hispanic/ Latino	M	55-60	Lung-LUL	Lung-LUL	Lung-LUL	No	Lung	2
	D9	04-P909354	Black/ AA	Hispanic/ Latino	M	65-70	Lung-LUL	Lung-LUL	Lung-LUL	Yes	Lung, kidney	33
	D9	04-P945456	Black/ AA	Not Hispanic/ Latino	F	50-55	Lung-LUL	Lung-LUL	Lung-LUL	No	Lung	7
	D13	04-P854921	White	Not Hispanic/ Latino	M	50-55	Lung-LUL	Lung-LUL	Lung-LUL	Yes	Multi-organ	8
	D11	04-P679042	White	–	M	70-80	Lung-LUL	Lung-LUL	Lung-LUL	Yes	Lung, kidney	7
	D13	04-P803149	White	Not Hispanic/ Latino	M	60-65	Lung-LUL	Lung-LUL	Lung-LUL	Yes	Multi-organ	33

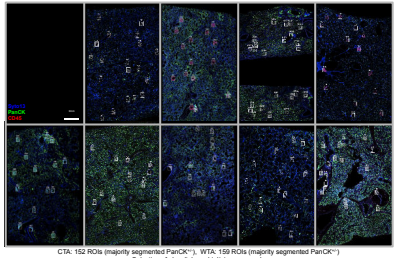

CTA: 152 ROIs (majority segmented PanCK$^{+/-}$), WTA: 159 ROIs (majority segmented PanCK$^{+/-}$)
Selection of alveoli, bronchial/airway, vessels

DSP revealed distinct cellular diversity in PanCK$^{+/-}$ compartments

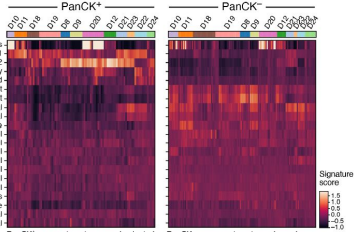

PanCK$^+$ compartments were dominated by either Type AT1 or AT2 cells, responsible for alveolar expansion and implicated in pulmonary fibrosis

PanCK$^-$ compartments showed a preference for fibroblasts, myofibroblasts, and vascular and lymphatic endothelial cells

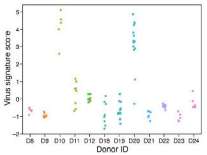

SARS-CoV-2 viral load between subjects

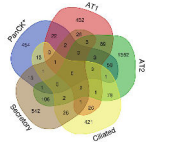

Gene classes upregulated in COVID-19$^+$, PanCK$^+$ AOIs. Interestingly, 111 of the 565 genes overlapped with genes expressed at higher levels in epithelial cell types with high ACE2 expression

Differential gene expression revealed coordinated immune and inflammatory response

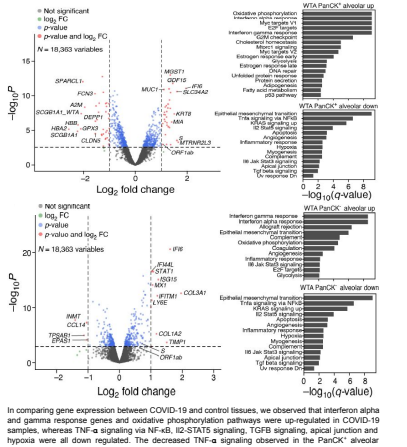

In comparing gene expression between COVID-19 and control tissues, we observed that interferon alpha and gamma response genes and oxidative phosphorylation pathways were up-regulated in COVID-19 samples, whereas TNF-α signaling via NF-κB, Il2-STAT5 signaling, TGFB signaling, apical junction and hypoxia were all down regulated. The decreased TNF-α signaling observed in the PanCK$^+$ alveolar compartment contrasts with the increased TNF signaling found in SARS-CoV-2 RNA containing epithelial cells, which could be explained by differential signaling in SARS-CoV-2 positive vs.negative epithelial cells.

Connecting with snRNA-seq atlas data

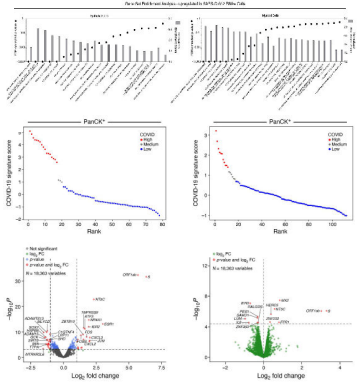

Differential analysis of GeoMx and snRNA-seq revealed upregulation in the PanCK$^+$ compartment of the chemokines CXCL2 and CXCL3, and of the immediate early genes EGR1, JUN, FOS, IER2, ZBTB10, and NR4A1. We also found that NT5C, encoding a nucleotidase with a preference for 5'-dNTPs, is consistently up-regulated in SARS-CoV-2 high in both PanCK+ and PanCK$^-$ conditions

Future directions

Correlating of gene/protein expressions in matched ROIs, as well as the sc/snRNA-seq from matched samples

Performing cluster analysis of AOIs based on clinical annotation of the tissue, viral load, and PanCK$^{+/-}$ segmentation

Confirm results with other spatial assays like CODEX or a more in-depth RNAscope to gain more spatial context for the snRNA-seq dataset

Acknowledgments

- Toni Marie Delorey, Carly G. K. Ziegler, Graham Heimberg, Rachelly Normand, Stephen J. Fleming, Ayshwarya Subramanian, Karthik Jagadeesh, Kushal Dey, Michal Slyper, Zohar Bloom-Ackerman, Andrea Ganna, James Gomez, Erica Normandin, Devan Phillips, Pritha Sen, Katherine J. Siddle, Victoria M. Tran, Shamsudheen K. Vellarikkal, Liat Amir-Zilberstein, Deepak S. Atri, Nick Barkas, Olga R. Brook, Prajan Divakar, Phylicia Dorceus, Jesse M. Engreitz, Donna M. Fitzgerald, Steven Gazal, Joshua Gould, John Grzyb, Tyler Harvey, Jonathan Hecht, Judit Jane-Valbuena, Michael Leney-Greene, Hui Ma, Cristin McCabe, Daniel E. McLoughlin, Eric M. Miller, Daniel T. Montoro, Christoph Muus, Mari Niemi, Robert Padera, Jenna Pfiffner-Borges, Christopher J. Pinto, Jacob Plaisted, Siddharth Raju, Melissa Rudy, Erroll H. Rueckert, Michelle Siciliano, Alex Sturm, Ellen Todres, Avinash Waghray, Shuting Zhang, Dan Zollinger, Lisa Cosimi, Rajat M. Gupta, Nir Hacohen, Alkes L. Price, Jayaraj Rajagopal, Purushothama Rao Tata, Timothy L. Tickle, Deborah Hung, Pardis C. Sabeti, Richard Novak, Robert Rogers, Don E. Ingber, Dejan Juric, Mehrtash Babadi, James Stone, Orr Ashenberg, Caroline B.M. Porter, Alex K. Shalek, Alexandra Chloé Villani for experimental work and data analysis

-Anita Hupalowska and Leslie Gaffney for help with figure preparation

-The National Institutes of Health (NIH) and the Human Tumor Atlas Network (HTAN) for funding this research

-**The patients and their families for their contribution in studying this disease**

KLARMAN CELL OBSERVATORY AT BROAD INSTITUTE · MGH · BWH · HTAN HUMAN TUMOR ATLAS NETWORK · NIH National Institutes of Health